

Provided for non-commercial research and education use.
Not for reproduction, distribution or commercial use.



This article appeared in a journal published by Elsevier. The attached copy is furnished to the author for internal non-commercial research and education use, including for instruction at the authors institution and sharing with colleagues.

Other uses, including reproduction and distribution, or selling or licensing copies, or posting to personal, institutional or third party websites are prohibited.

In most cases authors are permitted to post their version of the article (e.g. in Word or Tex form) to their personal website or institutional repository. Authors requiring further information regarding Elsevier's archiving and manuscript policies are encouraged to visit:

<http://www.elsevier.com/copyright>

available at www.sciencedirect.comjournal homepage: www.elsevier.com/locate/rmed

Breath-by-breath quantification of progressive airflow limitation during exercise in COPD: A new method

Shuyi Ma^a, Ariel Hecht^a, Janos Varga^a, Mehdi Rambod^a, Sarah Morford^a, Shinichi Goto^b, Richard Casaburi^{a,*}, Janos Porszasz^a

^a Rehabilitation Clinical Trials Center, Los Angeles Biomedical Research Institute at Harbor-UCLA Medical Center, 1124 W Carson Street, Torrance, CA 90502, USA

^b Tokyo Women's Medical University School of Medicine, Tokyo, Japan

Received 13 August 2009; accepted 19 October 2009

KEYWORDS

Expiratory flow limitation;
Chronic obstructive pulmonary disease (COPD);
Rectangular area ratio;
Spontaneous flow–volume curve;
Exercise;
Dynamic airway compression

Summary

During heavy exercise in chronic obstructive pulmonary disease (COPD), dynamic airways compression leads to a progressive fall in intrabreath flow. This is manifested by concavity in the spontaneous expiratory flow–volume (SEFV) curve. We developed a method to quantify the SEFV curve configuration breath-by-breath during incremental exercise utilizing a computerized analysis. The flow signal was digitized at 100 Hz. For each breath's SEFV curve, points of highest flow (\dot{V}_{\max}) and end-expiration (\dot{V}_{EE}) were identified to define a rectangle's diagonal. Fractional area within the rectangle below the SEFV curve was defined as the "rectangular area ratio" (RAR); $\text{RAR} < 0.5$ signifies concavity of the SEFV. To illustrate the utility of this method, time courses of RAR during incremental exercise in 12 healthy and 17 COPD individuals ($\text{FEV}_1 \text{ \%Pred.} = 39 \pm 12$) were compared. SEFV in healthy individuals manifested progressively more convex SEFV curves throughout exercise ($\text{RAR} = 0.56 \pm 0.08$ at rest and 0.61 ± 0.05 at peak exercise), but became progressively more concave in COPD patients ($\text{RAR} = 0.52 \pm 0.08$ at rest and 0.46 ± 0.06 at peak exercise). In conclusion, breath-by-breath quantification of SEFV curve concavity describes progressive shape changes denoting expiratory flow limitation during incremental exercise in COPD patients. Further studies are warranted to establish whether this novel method can be a reliable indicator of expiratory flow limitation during exercise and to examine the relationship of RAR time course to the development of dynamic hyperinflation.

© 2009 Elsevier Ltd. All rights reserved.

* Corresponding author. Tel.: +1 310 222 8200; fax: +1 310 222 8249.
E-mail address: casaburi@ucla.edu (R. Casaburi).

Introduction

Exercise intolerance in COPD patients is a common disabling complaint, which is particularly prominent in severe states.¹ An important determinant of exercise intolerance in patients with severe COPD is reduced ventilatory capacity, largely dictated by expiratory flow limitation (EFL) induced by elevated airway resistance and decreased elastic recoil.^{2–5}

The principal contributor of EFL is increased airway resistance as it propagates a cascade of changes in other modulators of airflow.⁶ Elevation of resistance lengthens the ventilatory time constants of the airways and necessitates increased intrathoracic pressure to drive flow.⁷ Higher pressures, in turn, augment gas compression and dynamic airway compression in the system.^{8–10} All of these factors lead to intrabreath reduction of flow^{2,4,8–10} manifesting in concave shape of the expiratory flow–volume curve – an indication that flow falls quickly as expiration proceeds.

Several approaches have sought to assess EFL during exercise.^{11–15} One method takes advantage of the fact that EFL exists when expiratory flow becomes independent of driving pressure so that flow does not increase when negative expiratory pressure (NEP) is applied at the mouth.¹³ Another method used to detect EFL is the forced oscillation technique, which relies on the concept that oscillatory pressure cannot pass through flow-limiting airway segments, thereby resulting in reduced apparent compliance and respiratory system input reactance.¹⁴ Although both NEP and forced oscillation techniques offer the means to quantify EFL during spontaneous breathing, the implementation of either method poses challenges for continuous quantification over the course of exercise. The forced oscillation technique requires complex instrumentation and special maneuvers.¹⁵ The NEP method does not allow assessment of breath-by-breath changes in EFL because the method necessitates comparison of the flow profiles of expirations with and without the application of NEP^{14,15} usually taken several breaths apart.

Given the fact that the expiratory limb of the flow–volume loop in a classic forced expiratory spirometry shows concavity in patients with obstructive airway disease and that concavity increases with severity of airflow obstruction, we hypothesized that EFL can be assessed *quantitatively* by examining the configuration of spontaneous expiratory flow–volume (SEFV) curves during rest and exercise on a breath-by-breath basis. In concept, this method does not require instructed breathing or modification of the usual procedures used in cardiopulmonary exercise testing.^{16,17} Information relevant to EFL can be gathered from the shape of SEFV curves because, as stated above, changes in the variables governing EFL (i.e. dynamic airway compression, gas compression, and lung unit time constants) are predictably reflected in intrabreath changes of flow. Moreover, in presence of EFL, flow rates of spontaneous expirations are governed by mechanisms similar to those influencing forced expirations,^{10,18} which have been previously used to characterize EFL.^{19–22} This implies that the shape of SEFV curves, especially the degree of its concavity, might be useful to quantify the progression of

EFL as exercise intensifies and the minute ventilation approaches breathing capacity.

In this methodological study, we aimed to develop computerized procedures to quantify the configuration of the spontaneous flow–volume profile on a breath-by-breath basis throughout the progression of incremental exercise, with special reference to the development of EFL in moderate to severe COPD patients. To gain a *preliminary* appreciation of the potential of this technique, and before comparing it with the above-mentioned known methods, we also compared the spontaneous expiratory flow–volume responses in a group of COPD patients and a group of age-matched healthy individuals. In addition, we examined the relation between the degree of SEFV curve concavity and measures of ventilatory limitation during exercise (i.e. \dot{V}_E/MVV).

Materials and methods

Study subjects

Seventeen men and women with the diagnosis of moderate to severe COPD were recruited. We included COPD individuals with forced expiratory volume in one second (FEV_1) $\leq 60\%$ of predicted as determined by the Hankinson reference equations.²³ We excluded individuals with acute respiratory exacerbation, those with diagnosis or symptoms of significant cardiac disease, those requiring chronic supplemental oxygen, those with resting oxygen saturation $< 89\%$ measured by pulse oximetry, and those who were exercise-limited by orthopedic or joint related diseases. Twelve healthy age-matched men and women were also recruited. All subjects signed the written informed consent for their participation in the study as approved by the Institutional Review Board of the Los Angeles Biomedical Research Institute at Harbor-UCLA Medical Center.

Pulmonary function and exercise tests

Each subject underwent resting spirometry (V_{max} 229, VIASYS SensorMedics, Yorba Linda, California, USA). COPD patients took 400 μg of albuterol by inhalation 20 min before testing in order to maximize bronchodilation. Maximum voluntary ventilation (MVV) was calculated as $FEV_1 \times 40$.²⁴ Lung volumes were measured using constant volume body plethysmograph (AutoBox 6200 D, VMax, SensorMedics). All pulmonary function tests fulfilled the ATS/ERS guidelines.²⁵

An incremental symptom-limited exercise test was performed on an electrically braked cycle ergometer (Ergoline 800, VIASYS SensorMedics) with a pedaling rate of 60 revolutions per minute. After 3 min of rest and 3 min of loadless pedaling, the work rate was increased by 5–15 watts (W) per minute in a ramp fashion (increment was 5 W/min if $FEV_1 < 1.0$ L, 10 W/min if $FEV_1 > 1.0$ L for the COPD patients; increment rate was 15 W/min for the healthy subjects). Participants were asked to continue to exercise up to the limit of tolerance, marked by inability (despite encouragement) to maintain pedaling frequency or

occurrence of intolerable shortness of breath. Shortness of breath and leg fatigue were assessed by the Borg category ratio scale every two minutes during exercise.²⁶

Data collection

Respiratory gas exchange (minute ventilation \dot{V}_E , oxygen uptake $\dot{V}O_2$, CO_2 output $\dot{V}CO_2$) were measured breath-by-breath by a commercial exercise system (Vmax Spectra, SensorMedics). The analog flow signal from the exercise system was digitized using a 16-bit A/D converter (WinDaq Acquisition Version 2.68, Dataq Instruments, Akron, Ohio, USA) at 100 Hz and stored on a personal computer for off-line analysis. Volume was derived by integrating the flow signal and was calibrated subsequently. The system calibration was demonstrated to be linear and to have zero intercept; therefore, a scalar multiplicative calibration factor was applied to adjust the computed expired volume from the flow signal.

Breath-cycle detection

Because flow toward the end of expiration often fluctuates around zero, it was unsatisfactory to apply a “crossing zero flow” criterion to discern the start and the end of a breath cycle. To overcome this, we moved the trigger-threshold to a small negative flow (−0.15 L/s). We defined the start of expiration as the point at which flow exceeded this threshold and was followed by a clear positive trend in the next 140 ms. Similarly, we defined the start of inspiration as the point at which flow exceeded this negative threshold, followed by a clear negative trend in the next 140 ms.

Computing the tidal volume during spontaneous respiration

Tidal volume calculation was accomplished by resetting the volume integration by using the Riemann Sums method at the start of each expiration.²⁷ This compensated for predictable inequalities in inspiratory and expiratory integrated volumes when the respiratory quotient differs from unity.

Computing the rectangular area ratio (RAR)

Spontaneous expiratory flow–volume curves were examined breath-by-breath, and a geometric analysis was performed by custom-made Sigma Plot 10.0 transform functions (SPSS Science, Chicago, IL). The geometric analysis was designed to examine the changes in the shape of the descending phase of the expiratory limb of the SEFV curves. The geometric analysis was based upon the identification of the intra-breath coordinates of two critical anchoring points: (A) the maximum spontaneous expiratory flow (\dot{V}_{max}) and (B) the point at which the expiratory flow takes a sharp decline signaling the beginning of inspiration (\dot{V}_{EE} , ‘end-expiratory flow’) (Fig. 1). V_{EE} was defined as the point associated with the greatest difference between the slopes of adjacent 20 ms segments of the flow–volume curve during the last 0.25 s of expiration. These two points were used to anchor a rectangle from which the breath-by-

breath rectangular area ratio (RAR) was calculated as a measure of concavity defined in the following way:

$$RAR = \frac{\int_{V@V_{max}}^{V@V_{EE}} \dot{V} dV - (\dot{V}_{EE} \times V_T)}{V_T(\dot{V}_{max} - \dot{V}_{EE})},$$

where $V@V_{max}$ and $V@V_{EE}$ are the volumes at \dot{V}_{max} and \dot{V}_{EE} , respectively and V_T is tidal volume. Values of RAR below 0.5 signify concavity while values above 0.5 signify convexity. This quantification makes comparisons of curvatures between different loops possible (Fig. 1).

All computer algorithms were developed using Sigma Plot transform functions (SPSS Science, Chicago, IL, USA) for breath detection and for the breath-by-breath determination of the parameters of the geometric analysis (RAR, \dot{V}_{max} , \dot{V}_{EE} and the relative position of \dot{V}_{max}). We report these variables in 30-s bin averages.

Statistical analysis

The results are presented as mean \pm SD in the text and tables and plotted as mean \pm SEM in the figures, unless noted otherwise. Group means were compared by unpaired two-tailed Student’s *t*-tests. To compare means between the two groups at different levels of exercise, we used two way repeated measures ANOVA with Holm-Sidak *post-hoc* analysis of variance to detect any individual significance. The statistical analyses were performed in SigmaStat 3.5 (SPSS Science). Statistical significance was accepted at $P < 0.05$.

Results

Subject characteristics and exercise tolerance

The demographic and resting spirometric findings of the study population are presented in Table 1. The resting pulmonary function showed a moderate to severe obstruction in the COPD patients. There were no statistically significant differences in age, height, and weight between the healthy and COPD groups.

Table 2 shows that, unlike the healthy individuals, COPD patients had a severely reduced exercise tolerance with marked ventilatory limitation as characterized by high end-exercise minute ventilation ($\dot{V}_{E peak}$) to MVV ratio ($\dot{V}_{E peak}/MVV$; $95 \pm 21\%$ vs. $54 \pm 8\%$ in the COPD patients vs. healthy individuals, respectively; $P < 0.05$).

Breath-cycle validation

As a validation procedure for breath cycle detection, each data set was visually inspected for accuracy and validity of breathing phase change and was manually corrected if necessary. Thus, we were able to count the number of false positive and false negative detections and calculate the sensitivity for detecting the start of expirations and inspirations. Among the 29 studies, the false positive detection rate for inspiration and expiration were $1.2 \pm 1.1\%$ and $1.9 \pm 1.3\%$, respectively. The false negative rate was $4.2 \pm 4.4\%$ for inspirations and $5.0 \pm 4.5\%$ for expirations.

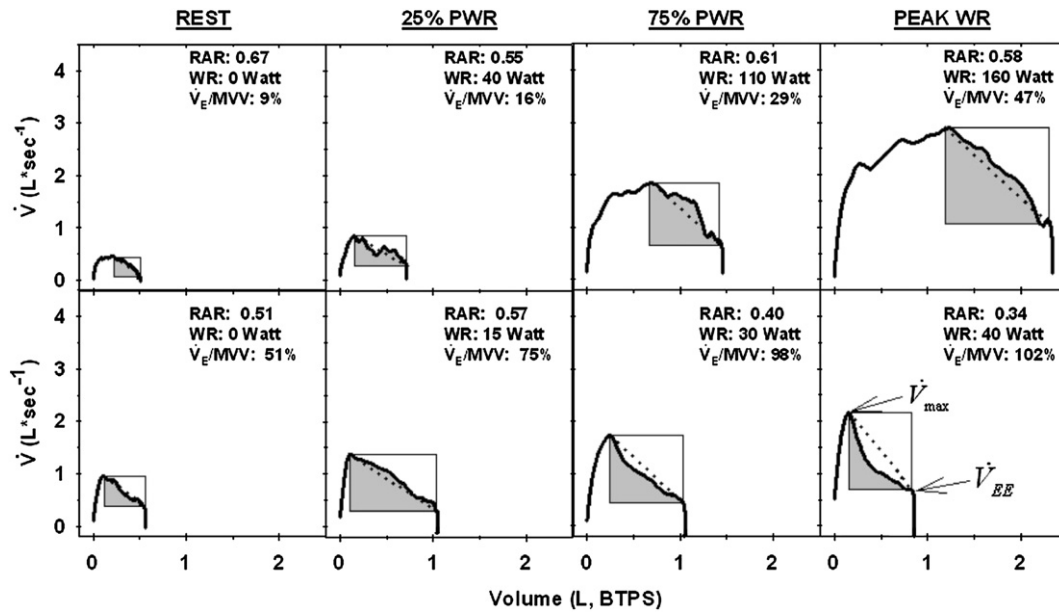


Figure 1 Progression of the spontaneous flow–volume (SEFV) curve configuration during incremental exercise. Top row: a healthy individual ($FEV_1 = 3.7$ L, 81% predicted). Bottom row: a severe COPD patient ($FEV_1 = 1.0$ L, 29% predicted). The shaded portion is the area used to calculate the rectangular area ratio (RAR); the triangle bounded by the dotted line, using the peak expiratory flow (\dot{V}_{max}) and the end expiratory flow (\dot{V}_{EE}) as anchor points, represents an RAR of 0.5, demonstrating no curvature. The healthy individual has an RAR that remains above 0.5, indicating SEFV curves with consistently convex profiles at all exercise levels. The COPD patient displays a declining RAR that achieves a minimum of 0.34 at peak exercise, indicating a markedly concave SEFV curve configuration as exercise progresses. Note that both the normal individual and the COPD patient increase intrabreath \dot{V}_{max} and \dot{V}_{EE} with progression of exercise and that the position of \dot{V}_{max} stays in the middle segment of the tidal volume in the healthy subject, while remaining within the first quarter of expiration in the COPD patient. PWR: peak work rate, WR: work rate, \dot{V}_E : minute ventilation, MVV: maximal voluntary ventilation calculated as $FEV_1 \times 40$.

The data presented below are derived from analysis after manual correction of all these errors in breath detection.

Progressive change in the shape of the spontaneous flow–volume curve during exercise

An animated sample demonstrating the occurrence of ‘buckling’ of the spontaneous expiratory flow–volume curve as exercise proceeds is presented in [Supplementary data](#). **Fig. 1** shows the expiratory phase of the flow–volume loop at rest and at 25%, 75%, and 100% of peak work rate in a typical healthy individual (upper row) and in a COPD patient (lower row). The shape of the expiratory limb of the SEFV curve at rest and during exercise in the healthy individual is *convex*, which is reflected by an $RAR \geq 0.5$ (**Fig. 1**, upper row). But in the COPD patient, the expiratory limb of the SEFV curve becomes *concave* at 75% peak work rate ($RAR = 0.4$) and shows more concavity at peak exercise ($RAR = 0.34$) (**Fig. 1**, lower row). Note that both the normal individual and the COPD patient increase intrabreath \dot{V}_{max} and \dot{V}_{EE} with progression of exercise and that the position of \dot{V}_{max} stays in the middle segment of the tidal volume in the healthy subject, while remaining within the first quarter of expiration in the COPD patient.

Fig. 2 illustrates the breath-by-breath analysis of the RAR, \dot{V}_{max} and \dot{V}_{EE} during the time course of unloaded cycling and incremental exercise in a healthy individual (upper panel) and a COPD patient (lower panel).

Table 1 Demographic and pulmonary function characteristics of the study subjects.

	Healthy (n = 12)	COPD (n = 17)
Age (yrs)	60 ± 9	63 ± 10
Height (cm)	169 ± 9	169 ± 10
Weight (kg)	74 ± 15	77 ± 12
FEV ₁ (L)	3.1 ± 0.8	1.1 ± 0.5*
FEV ₁ %Pred.	104 ± 13	39 ± 12*
FVC (L)	4.0 ± 1.0	2.8 ± 1.1*
FVC %Pred.	103 ± 14	77 ± 20*
FEV ₁ /FVC%	77 ± 4	40 ± 7*
MVV (L)	123.5 ± 31.1	43.7 ± 18.9*
PEF (L/s)	7.6 ± 1.9	3.3 ± 0.9*
TLC (L)	6.3 ± 1.3	7.1 ± 2.1
TLC %Pred.	108 ± 12.9	113 ± 17.8
FRC (L)	3.2 ± 0.7	4.8 ± 1.5*
FRC %Pred.	104 ± 23.1	146 ± 29.4*
RV (L)	2.3 ± 0.5	3.8 ± 1.4*
RV %Pred.	107 ± 16.8	163 ± 46.8*

*Pred. values in pulmonary function were calculated according to reference equations of Hankinson et al.²³ FEV₁: forced expiratory volume in the 1st s; FVC: forced vital capacity; MVV: maximum voluntary ventilation ($FEV_1 \times 40$)²⁴; PEF: peak expiratory flow; TLC: total lung capacity; FRC: functional residual capacity; RV: residual volume. * $P < 0.05$.

Table 2 Exercise tolerance and end-exercise ventilatory characterization (mean \pm SD).

	Healthy (n = 12)	COPD (n = 17)
Peak WR (W)	145 \pm 38	68 \pm 35*
$\dot{V}O_{2\text{ peak}}$ (L/min)	1.75 \pm 0.49	1.14 \pm 0.37*
$\dot{V}_{E\text{ peak}}$ (L/min)	66 \pm 19	40 \pm 14*
$\dot{V}_{E\text{ peak}}/\text{MVV}$ (%)	54 \pm 8	95 \pm 21*
V_T (L) at end-exercise	2.1 \pm 0.54	1.2 \pm 0.38*
RAR at end-exercise	0.61 \pm 0.05	0.46 \pm 0.06*

Peak WR: peak work rate in the incremental test; $\dot{V}O_{2\text{ peak}}$: peak oxygen uptake at end exercise; $\dot{V}_{E\text{ peak}}$: peak minute ventilation; \dot{V}_{E}/MVV : ratio of peak minute ventilation and maximal voluntary ventilation ($\text{MVV} = \text{FEV}_1 \times 40$)²⁴; RAR: rectangular area ratio; V_T : tidal volume; * $P < 0.05$.

Superimposed on these plots are smoothed curves calculated by a negative exponential smoothing method.²⁸ As seen in the upper panel of Fig. 2, in a healthy individual, the RAR smoothed curve of a healthy individual was above the 0.5 line at rest and throughout the exercise, reflecting the convexity of the SEFV curve during the test. Similarly, the lower panel of Fig. 2 shows that during unloaded cycling and early into the ramp exercise, the RAR smoothed curve in the COPD patient was at or above the 0.5 line, reflecting the convex shape of the expiratory limb of the SEFV curve. At about 5 min into the incremental exercise test, the RAR smooth curve fell below 0.5, signifying that the SEFV curve became concave. The RAR ultimately reached a nadir of 0.37 at peak exercise in this COPD patient. It can be seen that, at the time when the RAR smoothed curve fell below 0.5, \dot{V}_{max} reached about 1.5 L/s and \dot{V}_{EE} was appreciably above the resting level.

Fig. 3 shows, in both healthy and COPD individuals, the mean RAR plotted as a function of $\dot{V}_{E\text{ max}}/\text{MVV}$ at rest and during exercise: at 6, 4, and 2 min before end-exercise and at end-exercise. In healthy individuals (empty circles), RAR at 6 min before end-exercise dipped below the RAR at rest but subsequently progressively increased during the remainder of the test; RAR remained significantly above 0.5 throughout exercise. In marked contrast, average RAR of COPD patients at rest was slightly higher than 0.5 but then showed a continuous declining pattern throughout the exercise (average peak exercise value 0.46 ± 0.06). Fig. 3 also shows that, on average, the COPD patients used more than 90% of their respiratory reserve (i.e. they are ventilatory limited) at peak exercise.

We determined the number of COPD patients who showed average RAR during the last 30 s before exercise end of < 0.5 . We found that 14 out of 17 COPD patients manifested averaged RAR < 0.5 at end exercise, although in two of the 14 patients the nadir value was only slightly below 0.5 (approximately 0.49). We sought factors responsible for the failure to develop substantial concavity in these five COPD patients. These patients spanned the range of disease severity (i.e. $\text{FEV}_1\%$ predicted of 33, 34, 45, 52 and 56); hence, resting lung function does not seem to be a prime determinant of concavity in the SEFV curve during exercise. Two of the five had apparent ventilatory limitation (peak $\dot{V}_{E}/\text{MVV}\% = 103$ and 109) and three had substantial ventilatory reserve (mean $\dot{V}_{E}/\text{MVV}\% = 70 \pm 8$) at peak exercise.

Compared to the other 12 COPD patients who developed clear concavity during exercise, these five patients tended to be less dyspneic (Borg dyspnea score: 5.5 ± 1.9 vs. 4.8 ± 1.5) and tended to exhibit more leg fatigue (Borg leg score: 4.8 ± 2.0 vs. 5.8 ± 1.6) at peak exercise, though these differences did not reach statistical significance. None of the healthy individuals generated a RAR smoothed curve that fell below 0.5 at any point during exercise.

Discussion

We have shown that our novel, computerized algorithm allows non-invasive and unobtrusive detection and characterization of the genesis and development of progressive expiratory flow limitation that occurs during exercise in COPD patients. To the best of our knowledge, this is the first approach that allows quantification of EFL on a breath-by-breath basis by characterizing the profile of the SEFV curve. Unlike NEP measurement and the forced oscillation technique, our method does not require additional instrumentation beyond the flow sensor and digitizing equipment for the analog output of the flow sensor. The algorithm for this analysis might be implemented as a software module in preexisting computerized cardiopulmonary exercise systems. Furthermore, this method does not require instructed maneuvers and provides a fully quantitative, objective and dynamic measurement of developing flow limitation during exercise on a breath-by-breath basis.

In contrast to our new *quantitative* method, previous analyses of the shape of spontaneous flow–volume loop have been mainly limited to qualitative inspection. Morris and Lane first commented on the shape of the SEFV curve, noting that a non-sinusoidal expiratory flow pattern was indicative of obstruction, and pointed out that as EFL progresses the \dot{V}_{max} is reached earlier in the tidal breath.²⁹ Bardoczky and d'Hollander observed spontaneous flow–volume profiles of anaesthetized patients, pointing out the “bowing configuration” in the expiratory limb as an indication of diffuse obstruction.³⁰ Further, Baydur and Milic-Emili qualitatively assessed the flow–volume shape in association with the NEP method³¹ and observed SEFV curve concavity in patients with a high percentage of tidal volume exhibiting flow-limitation according to NEP; they reported that two-thirds of the patients with SEFV curve concavity had $>50\%$ of tidal volume exhibiting flow-limitation, and half of the patients showing concavity had $>70\%$ of tidal volume exhibiting flow limitation.

In our study, 14 of 17 COPD patients exhibited a value of RAR < 0.5 before peak exercise; however, there were five subjects with low FEV_1 who did not manifest substantial concavity in their SEFV curve. Conversely, in none of the normal subjects did the RAR smoothed curve drop below 0.5 at any point of exercise. By studying an age-matched control group, we have largely eliminated the possibility that the normally occurring decrease in elastic recoil with ageing might be associated with these configuration changes.

There is, however, a wide range of subjects who achieved ‘minimal’ RAR at peak exercise in the COPD group, and it is worthwhile to consider possible mechanisms of concavity that might lead to this variability. Several factors can be hypothesized to lead to concavity of the SEFV curve.

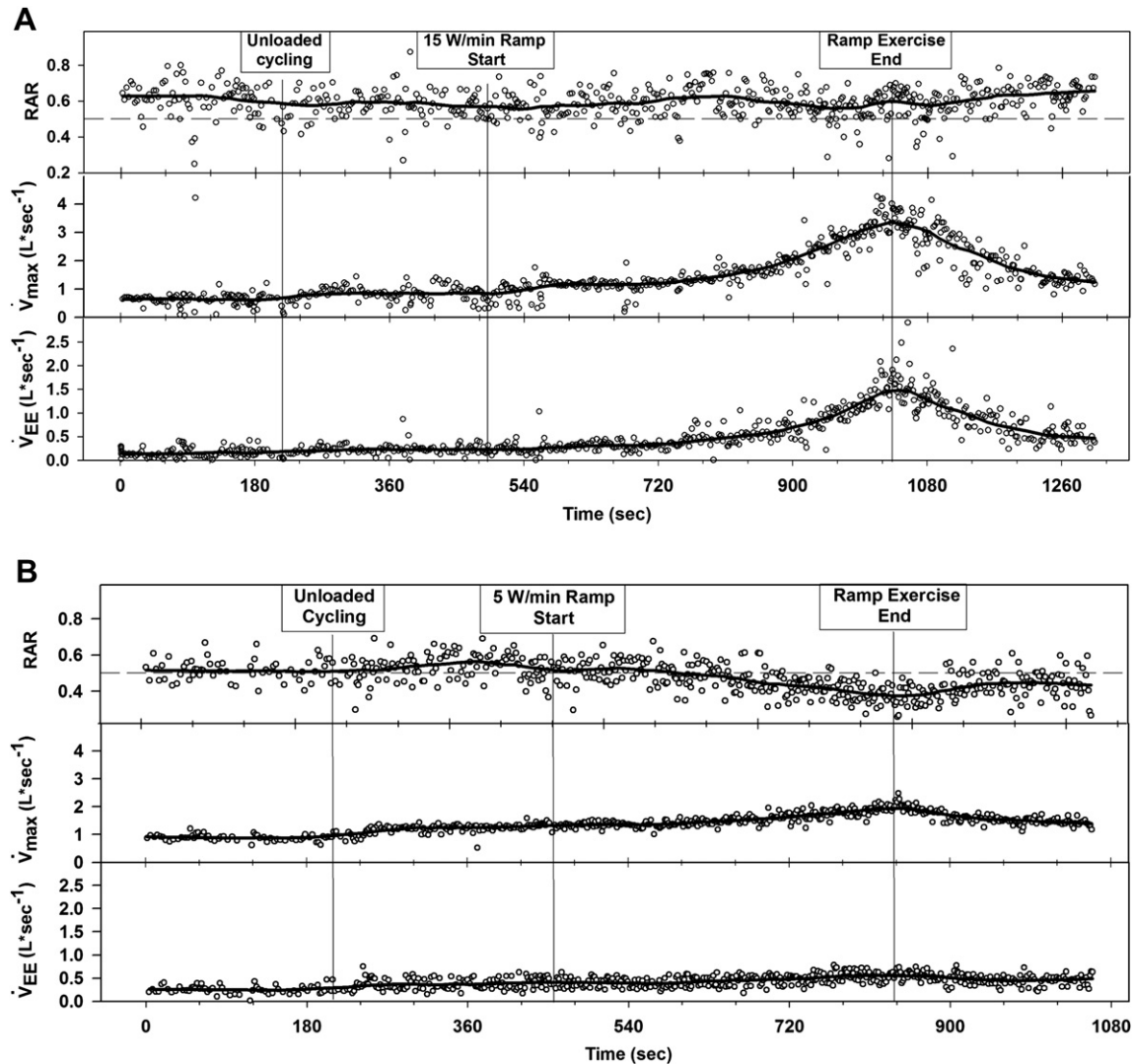


Figure 2 Breath-by-breath time course (open circles) of rectangular area ratio (RAR), peak expiratory flow (\dot{V}_{\max}) and end-expiratory flow (\dot{V}_{EE}) during an incremental exercise test. The heavy lines represent smoothed data (exponential method³²). Note that the ordinate scales for \dot{V}_{\max} and \dot{V}_{EE} are different in order to better represent the changes. Panel A: a healthy person (51 yrs, female, FEV₁: 2.72 L (98% predicted)). Panel B: a COPD patient (66 yrs, male, FEV₁: 1.02 L (29% predicted)).

The direct cause of concavity is a rapid drop in expiratory flow rate caused by dynamic airway compression.^{8,14,18} The drop in expiratory flow rate is exacerbated by rapid and shallow breathing adopted by COPD patients, which is at a frequency that limits effective ventilation to lung compartments with short time constants. Our data show that, as \dot{V}_{\max} rises during exercise, there is a shift of the position of the \dot{V}_{\max} to an earlier position in the expired volume, as previously observed by Morris and Lane.²⁹ Concavity might also result from gas compression, which largely depends on intrathoracic pressures achieved during expiration.⁹ Therefore, gas compression might occur in the presence of expiratory flow limitation.^{9,13} The configurational changes might also be consistent with an increasing role of active expiration in moderate to severe COPD patients. Further studies are warranted to determine the relative contribution of these potential mechanisms.

The "breath cycle determination" algorithm was one of the critical development tasks for this analysis. It is

generally agreed that using a slightly negative threshold is adequate to eliminate the influence of noisy flow signal toward the end of expiration. With the adoption of a slightly negative flow threshold to detect the beginning and end of expiration, post-detection visual inspection of approximately 14,000 flow-volume loops demonstrated that we achieved a low false positive and false negative rate in determining both inspirations and expirations. This finding indicates that in subsequent studies, visual confirmation of accurate breath detection by this algorithm will not be needed.

A potential limitation of RAR measurement technique is that noise in the expiratory flow signal interferes with accurate determination of the anchoring points (\dot{V}_{\max} and \dot{V}_{EE}), resulting in a rather significant scatter. Another possible reason for the variability in RAR is breath-by-breath physiologic variability in the exhalation, which results in various degrees of concavity or convexity of the expiratory limb of SEFV curve. Furthermore, we observed that the

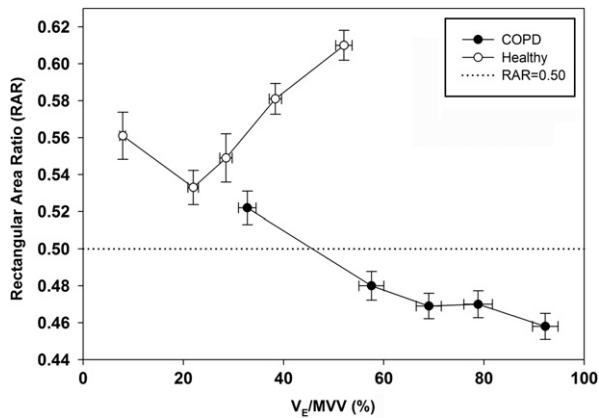


Figure 3 Rectangular area ratio (RAR) responses occurring at rest and as exercise limitation is approached during incremental exercise in healthy individuals ($n = 12$, open circles) and COPD patients ($n = 17$, closed circles). The abscissa presents mean \dot{V}_E/MVV at rest and at 6, 4, 2 and 0 min prior to end-exercise from left to right, respectively. RAR values of COPD patients are lower at rest and at all phases of exercise as compared to normal, non-obstructed subjects (repeated measures ANOVA $P < 0.01$). The RAR is significantly less than at rest starting 4 min before end-exercise (repeated measures ANOVA $P < 0.01$). In normal subjects, RAR is significantly higher than at rest starting two minutes prior to end of exercise (repeated measures ANOVA $P < 0.01$). The index of ventilatory limitation ($\dot{V}_E/MVV \times 100$) approaches a value of 100% in the COPD patients but not in the healthy individuals.

configuration of SEFV curve sometimes varies considerably between subsequent breaths that might lead to errors in determining the critical anchoring points for the calculation of RAR. Interestingly, the breath-to-breath variability was generally greater in healthy subjects than in COPD patients. We speculate that part of this variability might come from random changes in compliance or vibrations within the airways that is less characteristic in COPD. Additionally, the SEFV curve adopts more convex configuration in healthy subjects,²⁹ from which it is more difficult to separate the intrabreath peak- and end-expiratory flow, leading to variability in RAR calculations. In order to minimize the effect of breath-by-breath variability, we smoothed the breath-by-breath data using a single component exponential smoothing method³² which allowed characterization of trends. Another way of diminishing the effect of breath-to-breath configuration changes of the SEFV curve would be to average several consecutive breaths and calculate the RAR based on the averaged curves. A third way of dealing with this variability would be to exclude from further analysis RAR values that were outliers from the general trend. These methods might be explored in future studies.

In summary, breath-by-breath quantification of concavity of the expiratory limb of the SEFV curve by means of calculation of the RAR seems to be a suitable method for assessing development of EFL in COPD patients. Such configuration changes are the result of progressively active expiration and dynamic airway compression. Hence, it is plausible that measurement of RAR may have clinical implications in routine assessment of progressive flow limitation in COPD and may help to define critical

ventilatory limitation and dyspnea. Further studies are warranted to compare the results of this breath-by-breath quantification method with other methods of EFL determination such as the NEP method and the forced oscillation technique and to explore the validity and reliability of this method in stratification of COPD patients across the total spectrum of disease severity. It will also be important to examine the association of the SEFV configuration changes with dynamic hyperinflation as a possible mechanism of the observed SEFV concavity during exercise.

Conflict of interest

Authors have no conflict of interest to declare.

Acknowledgements

Dr. Casaburi occupies the Grancell/Burns Chair in the Rehabilitative Sciences. S. Ma, A. Hecht and S. Morford were participants of the Summer Fellowship Program of the Los Angeles Biomedical Research Institute at Harbor-UCLA Medical Center in 2005 and 2006. J. Varga was recipient of a stipend from the Hungarian Pulmonological Society. Dr. Goto produced the animated flow–volume curve presented in the online supplement while he spent his sabbatical at the Rehabilitation Clinical Trials Center.

Supplementary data

The animated mpg file was recorded from a subject performing a 5 W incremental exercise test to the limit of tolerance. The spirometry of this 61 yrs old female COPD subject showed, FEV₁: 0.98 L (38% predicted), FVC: 2.06 L (67% predicted) and FEV₁/FVC: 48%. This patient's test from a preliminary study was not part of the group of COPD patients presented in this article. Expiratory flow deflects upward and expiratory volume deflects rightward along the arbitrary scales. The 45 s animation replays the digitized data on about 1:10 time compression. At the start of the record the expiratory flow linearly decreases as expiration progresses. As exercise starts (at about 6 s into the animation) the peak expiratory flow of the spontaneous expiration starts increasing. A clear 'buckling' starts to occur in the middle segment of expiration (at about 18 s) lending a concave shape of the flow–volume curve. As a result of the 'peaked' maximal expiratory flow and the 'buckling' the spontaneous expiratory flow–volume curve starts to resemble to that seen during maximal effort spirometry. The incremental exercise ends at about 35 s. The buckling continues to be present during recovery. Note that the animated flow–volume loops are not aligned to total lung capacity and that wandering along the X axis is mainly due to changing differences in inspiratory and expiratory tidal volumes.

Supplementary data associated with this article can be found in the online version, at [doi:10.1016/j.rmed.2009.10.014](https://doi.org/10.1016/j.rmed.2009.10.014).

References

- Berry MJ. The relationship between exercise tolerance and other outcomes in COPD. *COPD* 2007;4:205–16.
- Milic-Emili J. Expiratory flow limitation: Roger S. Mitchell lecture. *Chest* 2000;117:219S–23S.
- O'Donnell DE. Ventilatory limitations in chronic obstructive pulmonary disease. *Med Sci Sports Exerc* 2001;33:S647–55.
- Potter WA, Olafsson S, Hyatt RE. Ventilatory mechanics and expiratory flow limitation during exercise in patients with obstructive lung disease. *J Clin Invest* 1971;50:910–9.
- Stubbing DG, Pengelly LD, Morse JL, Jones NL. Pulmonary mechanics during exercise in subjects with chronic airflow obstruction. *J Appl Physiol* 1980;49:511–5.
- Calverley PM, Koulouris NG. Flow limitation and dynamic hyperinflation: key concepts in modern respiratory physiology. *Eur Respir J* 2005;25:186–99.
- McNamara JJ, Castile RG, Ludwig MS, Glass GM, Ingram Jr RH, Fredberg JJ. Heterogeneous regional behavior during forced expiration before and after histamine inhalation in dogs. *J Appl Physiol* 1994;76:356–60.
- DeGraff Jr AC, Bouhuys A. Mechanics of air flow in airway obstruction. *Annu Rev Med* 1973;24:111–34.
- Ingram Jr RH, Schilder DP. Effect of thoracic gas compression on the flow–volume curve of the forced vital capacity. *Am Rev Respir Dis* 1966;94:56–63.
- Mead J, Turner JM, Macklem PT, Little JB. Significance of the relationship between lung recoil and maximum expiratory flow. *J Appl Physiol* 1967;22:95–108.
- Dellaca RL, Rotger M, Aliverti A, Navajas D, Pedotti A, Farre R. Noninvasive detection of expiratory flow limitation in COPD patients during nasal CPAP. *Eur Respir J* 2006;27:983–91.
- Hyatt RE. The interrelationships of pressure, flow, and volume during various respiratory maneuvers in normal and emphysematous subjects. *Am Rev Respir Dis* 1961;83:676–83.
- Koulouris NG. Negative expiratory pressure: a new tool. *Monaldi Arch Chest Dis* 2002;57:69–75.
- Dellaca RL, Santus P, Aliverti A, Stevenson N, Centanni S, Macklem PT, et al. Detection of expiratory flow limitation in COPD using the forced oscillation technique. *Eur Respir J* 2004;23:232–40.
- Farre R, Navajas D. Assessment of expiratory flow limitation in chronic obstructive pulmonary disease: a new approach. *Eur Respir J* 2004;23:187–8.
- ATS/ACCP. Statement on cardiopulmonary exercise testing. *Am J Respir Crit Care Med* 2003;167:211–77.
- Palange P, Ward SA, Carlsen KH, Casaburi R, Gallagher CG, Gosselink R, et al. Recommendations on the use of exercise testing in clinical practice. *Eur Respir J* 2007;29:185–209.
- Dawson SV, Elliott EA. Wave-speed limitation on expiratory flow—a unifying concept. *J Appl Physiol* 1977;43:498–515.
- Landau LI, Taussig LM, Macklem PT, Beaudry PH. Contribution of inhomogeneity of lung units to the maximal expiratory flow–volume curve in children with asthma and cystic fibrosis. *Am Rev Respir Dis* 1975;111:725–31.
- Mead J. Analysis of the configuration of maximum expiratory flow–volume curves. *J Appl Physiol* 1978;44:156–65.
- Pedersen OF, Ingram Jr RH. Configuration of maximum expiratory flow–volume curve: model experiments with physiological implications. *J Appl Physiol* 1985;58:1305–13.
- Tien YK, Elliott EA, Mead J. Variability of the configuration of maximum expiratory flow–volume curves. *J Appl Physiol* 1979;46:565–70.
- Hankinson JL, Crapo RO, Jensen RL. Spirometric reference values for the 6-s FVC maneuver. *Chest* 2003;124:1805–11.
- Campbell SC. A comparison of the maximum voluntary ventilation with the forced expiratory volume in one second: an assessment of subject cooperation. *J Occup Med* 1982;24:531–3.
- Miller MR, Hankinson J, Brusasco V, Burgos F, Casaburi R, Coates A, et al. Standardisation of spirometry. *Eur Respir J* 2005;26:319–38.
- Borg GA. Psychophysical bases of perceived exertion. *Med Sci Sports Exerc* 1982;14:377–81.
- Anton H. *Calculus: A new horizon*. New York: Wiley; 1999. p. 324–7.
- Spliid H. Monitoring medical procedures by exponential smoothing. *Stat Med* 2007;26:124–38.
- Morris MJ, Lane DJ. Tidal expiratory flow patterns in airflow obstruction. *Thorax* 1981;36:135–42.
- Bardoczky GI, d'Hollander A. Continuous monitoring of the flow–volume loops and compliance during anesthesia. *J Clin Monit* 1992;8:251–2.
- Baydur A, Milic-Emili J. Expiratory flow limitation during spontaneous breathing: comparison of patients with restrictive and obstructive respiratory disorders. *Chest* 1997;112:1017–23.
- What is exponential smoothing? In: NIST/SEMATECH e-handbook of statistical methods; 2006.